

# Interactions and Ordering of Ionic Liquids at a Metal Surface

Ana C. F. Mendonça, Patrice Malfreyt, and Agílio A. H. Pádua\*

Institut de Chimie de Clermont-Ferrand, Université Blaise Pascal & CNRS, 63171 Aubière, France

**ABSTRACT:** An atomistic force field for ionic liquids interacting with a metal surface is built on the basis of quantum methods. Density functional calculations of alkylammonium cations and alkylsulfonate anions interacting with a cluster of iron atoms were performed, at a series of distances and orientations, using the M06 functional that represents noncovalent interactions. A site-site potential function was then adjusted to the BSSE-corrected DFT interaction energies. Finally, the polarization of the metal by the ions was taken into account using induced dipoles to reproduce the interaction energy between charges and a conductor surface. When combined with a molecular force field for the ionic liquid and a suitable potential for metals, our model allows the computer simulation of heterogeneous systems containing metal surfaces or nanoparticles in the presence of ionic liquids. Our aim is to study tribological systems with ionic lubricants. We report molecular dynamics results on the structure of the interfacial layer of several alkylammonium alkylsulfonate ionic liquids at a flat iron surface, including analyses of the positional and orientational ordering of the ions near the surface, and charge density profiles. Both anions and cations are found in the first ordered layer of ions near the surface, with the oxygen atoms of the sulfonyl groups interacting more strongly with the metal. The interfacial layer is essentially one ion thick, except for very short chain ionic liquids in which a second layer is observed. The effects of different lengths of the nonpolar alkyl side chains on the cation and the anion are different: whereas butyl chains on the sulfonate anions tend to be directed away from the surface, those on ammonium cations lie more parallel to the surface.

## INTRODUCTION

In this work, we describe the molecular interactions in a system composed of an ionic liquid at the interface with a metal, in order to provide an atomistic force field for use in molecular simulations. At the present state of knowledge, the interactions within a room-temperature ionic liquid can be described by atomistic force fields available in the literature,<sup>1–8</sup> and the forces between atoms in a metal can also be described by specific nonadditive models such as Finnis–Sinclair potentials.<sup>9</sup> However, the interactions between the large and complex molecular ions of the ionic liquid and a metal have only been described in detail in one previous publication of our group<sup>10</sup> concerning the stabilization of ruthenium nanoparticles in imidazolium ionic liquids. This interaction model is based on recent DFT methods that correctly describe nonbonded interactions and includes polarization of the conducting surface. Here, we apply this new methodology to develop an interaction model between alkylammonium alkylsulfonate ionic liquids, which are environmentally acceptable ionic lubricants,<sup>11,12</sup> and iron surfaces. This type of specific model is of interest for the study of tribological or electrochemical systems, for which no reliable or satisfactory models exist. The methodology proposed to construct the interaction model is general for molecular or ionic species interacting with conducting surfaces and can be applied in a variety of problems in physical chemistry, nanosciences, or materials science.

In a tribosystem, lubrication is one of the key aspects influencing friction and wear by preventing the direct asperity–asperity contact and by lowering contact temperature. The search for high-performance lubricants is an active field<sup>13–15</sup> that includes the study of new fluid compounds that can be designed in view of applications. In recent years, ionic liquids have been identified as potential lubricants<sup>16,17</sup> due to their unique properties,<sup>18</sup> which include negligible vapor pressure,

nonflammability, high thermal-oxidative stability, and reasonable viscosity-temperature behavior,<sup>19</sup> all important characteristics to take into account when choosing a lubricant. Furthermore, the strong electrostatic interactions of ionic liquids<sup>19</sup> enable the formation of adsorbed films, contributing to the reduction of friction and wear. The use of ionic liquids as base-oil additives can also enhance the antiwear behavior of the lubricant by preventing some tribochemical reactions at the surface such as corrosion and oxidation.<sup>20,21</sup>

In the present study, ionic liquids with suitable ecotoxic and biodegradable properties and appropriate tribological characteristics were chosen as potential lubricant oils. The chemical structures are based on tetraalkyl-ammonium cations<sup>22</sup> combined with different families of anions including alkyl-sulfonate and bis(trifluoromethanesulfonyl)amide, or bistriflamide. The choice of the ammonium cations is linked to their performance as lubricants or additives when associated with bistriflamide<sup>22</sup> anions,  $\text{NTf}_2^-$ . Sulfonate anions were preferred due to their low environmental impact when compared to fluorinated anions,<sup>11,12</sup> which are very common in ionic liquids. Some combinations of anions and cations may not be liquid at room temperature. Certain properties of ionic liquids, such as melting point, solubility, and viscosity, are strongly dependent on the molecular structures and on the nature and length of the alkyl side-chains,<sup>23</sup> so by changing these side groups it is possible to fine-tune these relevant properties for applications as lubricants.

The nature of the molecular interactions occurring at the solid–liquid interface has great influence on the performance of a lubricant. The aim of this study is to describe at the molecular level the organization and dynamics of the ions at a metal

Received: June 1, 2012

Published: July 25, 2012



surface using molecular dynamics simulation (MD). This class of methods provides molecular insights toward explaining properties such as friction, lubrication, and wear by analyzing the tribosystems on the nanoscale.<sup>24,25</sup> Although in some situations quantitative predictions can be attained, the most relevant information is usually of a qualitative nature, in terms of trends and structure–property relations that can guide the choice of compounds for lubricants.

The main difficulty in simulating systems composed of a solid and a liquid is often the description of the solid–liquid interactions. In the present study, an innovative model for handling interaction between ionic liquids and an iron surface was developed from first principles, following the method set up by Pensado and Pádua.<sup>10</sup> This method accounts for the polarization effect of electrostatically charged entities near a conducting surface, a contribution that is expected to be important for the systems studied here. Several molecular simulation studies of ionic liquids near conducting surfaces, such as metals or graphene-like surfaces, have been published, but most of them<sup>26–28</sup> totally omit these polarization terms and the results therefore may be far from reality. The modeling of ions near metal or graphite electrodes using simpler representations (hard bodies with point charges)<sup>29,30</sup> shows that the inclusion of polarization is crucial in the reproduction of the metal charge fluctuations that depend on the nearby liquid structure. Also, the ordering of the liquid layer will have great influence on the metal polarization effect.

Several groups studied the structure of ionic liquids at conducting surfaces using experimental methods. Surface-spectroscopic measurements performed by Baldelli<sup>31</sup> at a platinum surface showed that the ions form an interfacial layer with a thickness of approximately 5 Å, which corresponds roughly to one ion-pair thickness. Charge ordering does not extend far into the liquid due to the strong screening effects of that ionic medium. Atkin and co-workers<sup>18</sup> detected a very strong first solvation layer at a gold surface using atomic force microscopy, and while discernible ordering can be observed up to three or four layers, the ordering of these is more significantly damped than in nonconducting substrates.

The present manuscript is divided in two main parts: First, we describe the development of an interaction model between ionic liquids composed of alkyl-ammonium cations and alkyl-sulfonate anions, and an iron surface, based on quantum chemical calculations and including the polarization of the conducting surface. Second, we report results on the molecular simulation of the ionic liquids at a surface of Fe, namely, the positional and orientational ordering of the ionic liquids as well as electrostatic charge distributions. These results are interpreted in terms of the molecular structure of the ions.

## ■ INTERACTION MODEL

Three kinds of molecular interactions have to be taken into account in an ionic liquid–metal system: ion–ion, metal–metal, and metal–ion, the last ones being the most complex to describe. The ion–ion interactions were represented by a molecular force field based on the OPLS-AA model,<sup>32,33</sup> specifically parametrized for the ionic liquids studied in this work.<sup>2,4</sup> For the metal–metal interaction, a Finnis–Sinclair potential<sup>9</sup> was used. This potential functional form is derived from quantum calculations and describes the bonding of metal atoms in terms of the local electronic density. The potential is therefore nonadditive, and parameters for a bcc iron crystal structure were obtained from Watanabe and et al.<sup>34</sup>

The interactions between the ionic liquids and an Fe(001) surface were determined from quantum calculations using density functional theory (DFT). The M06-L density functional proposed by Zhao and Truhlar<sup>35</sup> was chosen since it provides a correct description of long-range and nonbonded energies of systems containing both main-group atoms and transition metals.<sup>10</sup> In order to optimize the computational time and construct a transferable model, which should be able to describe families of ionic liquids, the ionic system composed by alkyl-ammonium cations and alkyl-sulfonate anions was split into three fragments: butane ( $C_4H_{10}$ ), tetramethylammonium ( $[N_{1111}]^+$ ), and methylsulfonate ( $[CH_3SO_3]^-$ ). The transferability of parameters, known as the *LEGO approach*,<sup>36</sup> is based in the assumption that the electron density distribution in a given molecular fragment is similar for different molecules and different locations of the fragment, which is a reasonable approximation if the fragments are carefully chosen. Present knowledge about the structure and charge distribution of ionic liquids supports the existing rationale for defining the fragments, by separating charged head groups and nonpolar alkyl side chains. Then, by assembling different molecular fragments, one can build a great variety of cation–anion combinations. The interaction energy of each fragment was sampled at different distances and different orientations from a (001) surface of a bcc cluster containing 21 atoms (Figure 1).

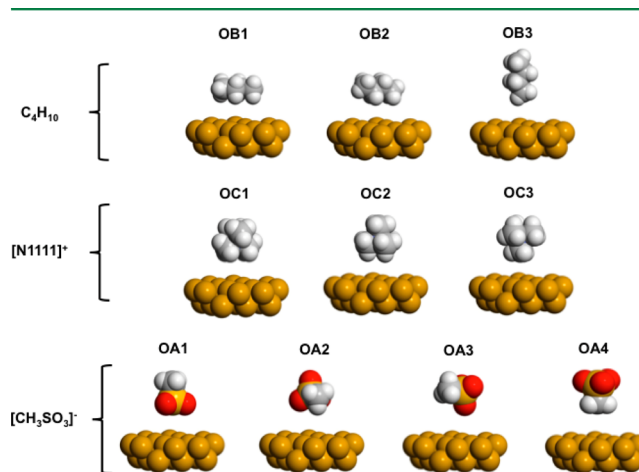


**Figure 1.** Orientations of the fragments of ionic liquid in respect to a 21 atom Fe(001) cluster.

All of the DFT calculations were carried out using the Gaussian 09<sup>37</sup> software. For the ionic fragments, we employed a triple- $\zeta$  valence basis set, TZVP<sup>38</sup> and, for iron, an effective core potential set from the Stuttgart/Cologne group,<sup>39</sup> ECP10MHP. Conversion problems led us to proceed by obtaining an initial approximation with the LSDA<sup>40</sup> functional and the LanL2DZ<sup>41,42</sup> basis set for both metal and liquid. Iron is ferromagnetic; therefore, open-shell calculations were performed with a spin multiplicity  $M = 2S + 1$  ( $S$  represents the number of unpaired electrons) of 2.9 per atom according to Frauenheim et al.<sup>43</sup> The basis set superposition error was corrected through the counterpoise technique.<sup>44</sup>

The potential energy between the fragments of the ionic liquid and the metal cluster is shown in Figure 2, where the points represent DFT energy calculations for each ion fragment at different orientations and distances from the metal cluster. It can be seen that the adsorption energy of butane on Fe(001) (Figure 2a) in the most favorable orientation (in red) is  $-33$  kJ

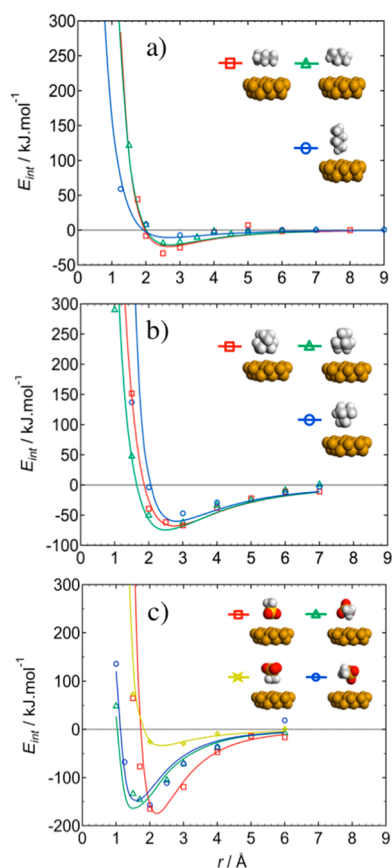


**Figure 2.** Interaction energy of the different fragments of ionic liquid at a series of distances and four orientations from a 21-atom cluster of Fe(001): (a) butane, (b) tetramethylammonium, (c) methylsulfonate.

$\text{mol}^{-1}$ , corresponding to a physisorption mechanism,<sup>45</sup> where the attraction between the adsorbed species and the surface arises from van der Waals forces. We could not find experimental values of adsorption energies of butane on iron, but it is known that the adsorption at Ni(111)<sup>46</sup> is  $-37 \text{ kJ}\cdot\text{mol}^{-1}$ . Interactions between adsorbed butane molecules can account for about 25% of the total adsorption energy;<sup>47</sup> therefore, we can conclude that our calculation is a very reasonable prediction.

For the methylsulfonate fragment, the binding energy to the iron surface is larger than that of the other molecules, especially in the orientation labeled in red where the oxygens are directed toward the surface. This reveals the possible presence of a component of chemisorption<sup>48</sup> between the oxygens and sulfur of the fragment and the iron atoms. Such a strong sorption is not seen when the methyl group is directed toward the cluster.

In order to use the results of interaction energies in a molecular simulation, a function must be chosen to represent the potential energy surface in terms of distance and orientation. We decided to use an atom–atom model, in which the overall energy of the fragment of ionic liquid and the metal cluster is decomposed into site–site contributions. As such, each energy point for a given distance and orientation in Figure 2 is the result of all of the pairwise interactions between each site of the ionic liquid fragment and each metal atom. This allows the representation of flat or arbitrary surface topologies. The number of different sites cannot be too large since we start from a data set of about 30–40 points of discrete energies for the series of distances and orientations, for each fragment. This

data set allows only the definition of so many parameters. We therefore chose not to represent H atoms explicitly on the fragments of the ionic liquid but, instead, to include them in united-atom sites. The model of the ionic liquid, for the purpose of interactions with the metal, is therefore a united-atom model. (However, when calculating ion–ion interactions the full, all-atom force field is kept). Specifically, the interactions between butane and the Fe cluster are represented by two kinds of site: one for  $-\text{CH}_3$  groups and another for  $-\text{CH}_2-$  groups. The interactions of tetramethylammonium are represented by one site for the N and four sites for methyl groups attached to the positively charged central atom. Methylsulfonate is represented by five sites, i.e., explicit O and S atoms, and one united  $-\text{CH}_3$  site connected to the negative headgroup. Due to the very different chemical environments of the methyl groups in butane or in the cation and anion considered, it is normal that the parameters describing this group are not the same. A good fit to the curves in Figure 2 is obtained using site–site potential functions of the type  $n - m$ <sup>49</sup> as in eq 1.

$$u(r) = \frac{E_0}{(n-m)} \left[ m \left( \frac{r_0}{r} \right)^n - n \left( \frac{r_0}{r} \right)^m \right] + \frac{q_i q_j}{r} \quad (1)$$

The parameters obtained are summarized in Table 1.

**Table 1.** Parameters of Interaction Obtained by the Fitting, to Be Used in the Molecular Dynamics Simulations of the System Composed by Ionic Liquid Confined between the Two Iron Surfaces

fragment	atom	$E_0$ (kJ mol <sup>-1</sup> )	$r_0$ (Å)	$n$	$m$
$\text{CH}_3\text{SO}_3^-$	O	17.226	2.258	7	6
	S	11.018	3.402	7	6
$(\text{CH}_3)_4\text{N}^+$	$\text{C}_\text{S}$	0.573	3.864	7	6
	N	1.999	5.166	6	5
	$\text{C}_\text{N}$	1.480	4.277	6	5
$\text{C}_4\text{H}_{10}$	$\text{C}_{2\text{H}}$	2.069	3.116	7	6
	$\text{C}_{3\text{H}}$	0.530	4.654	7	6

The polarization of the metal surface was taken into account in the metal–liquid force field by adding a specific term to the potential energy. A polarizable metal surface was obtained by employing a Drude-rod concept developed by Iori and Corni,<sup>50</sup> by the addition of an embedded dipole into each metal atom, which is free to rotate in response to the local electric field. It was demonstrated that this technique reproduces the interaction energy of charges with conducting surfaces, in a similar manner to induced dipoles, while avoiding instability issues. The opposite charges ( $q$ ) are separated by a distance ( $l_0$ ) and have the same mass ( $m$ ). The parameters used herein are  $l_0 = 0.7 \text{ Å}$ ,  $m = 0.5 \text{ au}$  and  $q = 0.3e$ .

The final system studied here is formed by slabs of iron atoms in contact with a central slab of ionic liquid, as shown in Figure 3. Three main types of interaction potentials are used: (i) Ion–ion interactions within the ionic liquid are described by a classical force field with intramolecular terms including harmonic covalent bonds, harmonic valence angles, and cosine series for torsion energy profiles around dihedral angles; nonbonded intermolecular forces are given by Lennard-Jones atomic sites and fixed electrostatic point charges. (ii) Metal–metal interactions within the iron slabs are represented by a Finnis–Sinclair potential. (iii) Interactions between the metal



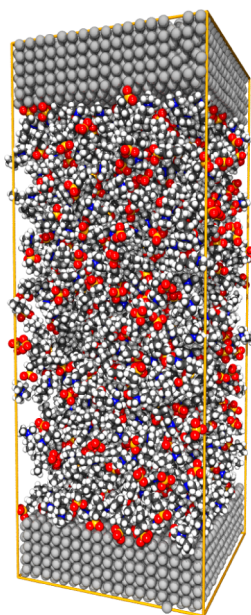


**Figure 3.** Snapshot of the equilibrated simulation box composed of 500 ion pairs confined between two surfaces of bcc iron, with tridimensional periodic conditions.

and the ionic liquid are described by the  $n - m$  potential functions developed here, between each metal atom and each site on the ions, augmented by the electrostatic forces of the point partial charges on the atomic sites of the ions and the Drude dipoles on the metal atoms that represent the polarization of the surface. The Drude dipoles have no effect on the lattice structure of the metal slabs at the temperatures of this study.

### MOLECULAR DYNAMICS SIMULATION

A slab of 500 ion pairs was simulated between surfaces of bcc iron by molecular dynamics using the DL\_POLY package.<sup>51</sup> The simulation box is a rectangular parallelepiped of dimensions  $L_x L_y L_z$  ( $L_x = L_y = 49$  Å,  $L_z = 120$  Å) with periodic conditions applied in the three dimensions (Figure 3). All simulations were performed at 500 K in order to improve statistical sampling, since due to the high viscosity of ionic liquids, convergence of the molecular dynamics trajectories is too slow at room temperature for practical purposes.<sup>52</sup> The initial configuration was a low-density lattice containing only the ionic liquid that was equilibrated at constant pressure (1 atm) with a time step of 1 fs in order to reach the correct density of the bulk liquid. Then, the metallic surfaces, each composed of 2890 Fe atoms in the bcc structure, were inserted. The dimension of the resulting box was increased along the  $z$  axis by placing 60 Å of empty space on the external sides of the surfaces. This procedure is necessary in order to apply the three-dimensional Ewald summation method in a slab geometry using the 3D periodic boundary condition.<sup>53</sup>

After equilibration of the system, a simulation run of 2 ns was executed with a time step of 2 fs, at constant  $NpT$  regulated by a Nosé–Hoover thermostat and barostat. Long-range electrostatic interactions were handled through the Ewald summation technique, using a real-space cutoff of 14 Å. The number of wave-vectors considered in the reciprocal space were of  $k_x = k_y = 5$  and  $k_z = 23$ , yielding a relative accuracy better than 0.001 in the calculation of the electrostatic energy. Configurations from

the production runs were stored every 1000 time steps for subsequent analyses.

Three ionic liquids with different alkyl chain lengths in the anion or in the cation were simulated: 1-butyl-1,1,1-methylammonium metanesulfonate  $[N_{1114}][C_1SO_3]$ , 1-butyl-1,1,1-methylammonium butanesulfonate  $[N_{1114}][C_4SO_3]$ , and 1-butyl-1-ethyl-1,1-methylammonium butanesulfonate  $[N_{1124}][C_4SO_3]$ , illustrated in Figure 4.

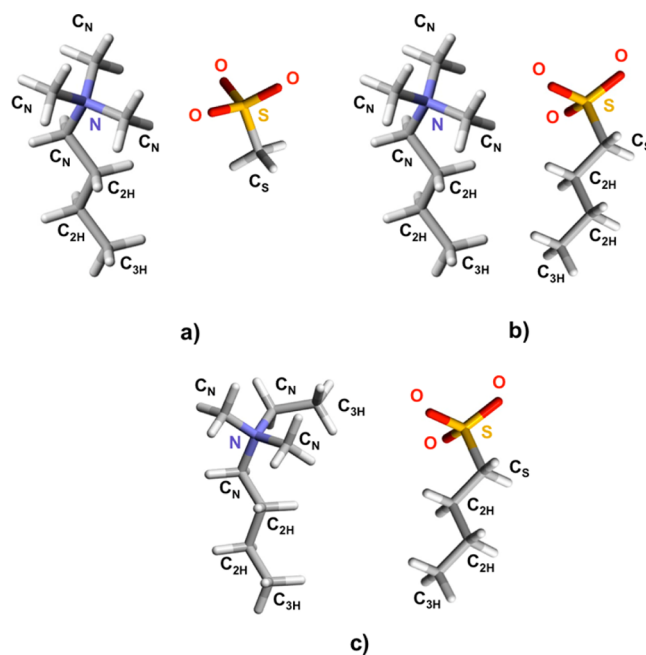


**Figure 4.** Molecular structures of the simulated ionic liquids: (a) 1-butyl-1,1,1-methylammonium butanesulfonate  $[N_{1114}][C_4SO_3]$ , (b) 1-butyl-1,1,1-methylammonium metanesulfonate  $[N_{1114}][C_1SO_3]$ , and (c) 1-butyl-1-ethyl-1,1-methylammonium butanesulfonate  $[N_{1124}][C_4SO_3]$ .

### RESULTS AND DISCUSSION

The first results from MD simulations we analyze are the structure of the ions near the surface, through number-density profiles for atoms of  $[N_{1114}][C_1SO_3]$ ,  $[N_{1114}][C_4SO_3]$ , and  $[N_{1124}][C_4SO_3]$ , presented in Figure 5. The oxygen atoms (O) and the sulfur atom (S) are representative of the headgroup of the alkyl-sulfonate anion. The nitrogen atom (N) is representative of the positive headgroup of the alkyl-ammonium cation. Finally, the terminal carbon atoms ( $C_{3H}$ ) represent the position of the longer alkyl chains in either anions or cations.

In the local density profiles of ionic liquid  $[N_{1114}][C_1SO_3]$ , two layers of anion headgroups are observed, clearly marked by the peaks of S and O atoms. Logically, O atoms approach closer to the surface. The distance between the first two peaks of O density is 5.0 Å; therefore, this really corresponds to two layers of anions, not to distances between O atoms within the same sulfonyl group, which is 2.4 Å. Only one structured layer of cation headgroups is perceived through the strong peak of N atoms, at distances from the surface that are slightly larger than that of S atoms from the anion. The most probable positions of the terminal C atoms in the butyl side chain of the cations correspond to a second peak, which is slightly higher than the first and appears further away from the surface than the charged

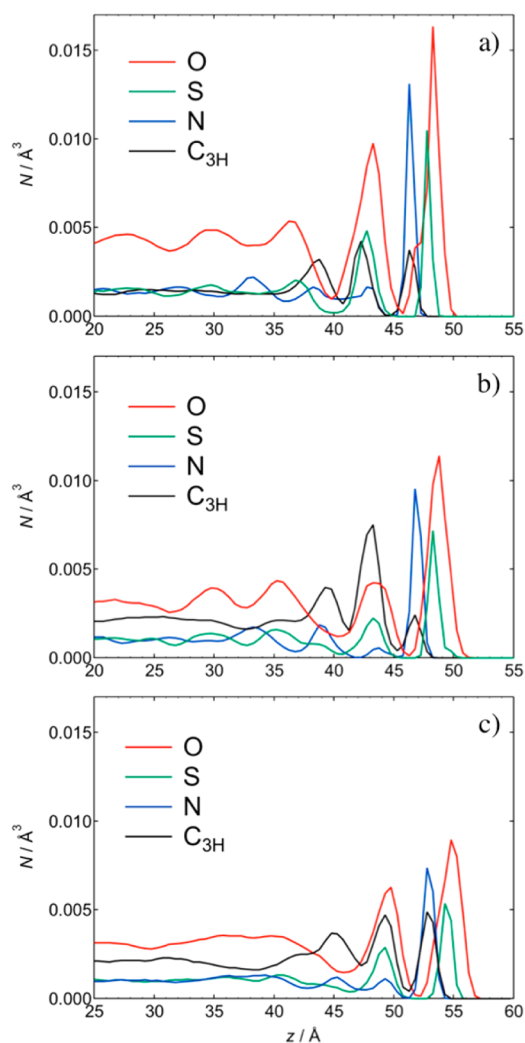


**Figure 5.** Atomic density profiles near the interface with Fe for the ionic liquids: (a)  $[N_{1114}][C_1SO_3]$ , (b)  $[N_{1114}][C_4SO_3]$ , and (c)  $[N_{1124}][C_4SO_3]$ . The red curve and the green curve represent the oxygen atoms and sulfur atoms of the headgroup of the anion, respectively. The blue curve represents the nitrogen atoms of the headgroup of the cation, and the black curve represents the terminal carbon atoms of the butyl side chains of either the anion or the cation.

headgroups. The interfacial layer of this ionic liquid is composed of anion and cation headgroups separated by 2 Å,

with a second, less-ordered layer of anions. Separation between cations and anion layers is significantly smaller than their diameters; therefore, both types of ion are present at the interface, with the alkyl chains preferentially directed toward the bulk liquid.

Overall similar features are seen in the atomic density profiles of the other two ionic liquids, which have longer alkyl side chains. The main difference from the ionic liquid discussed above is a reduction in the height of the peaks arising from the anion and cation headgroups. In  $[N_{1114}][C_4SO_3]$ , the second peak of terminal atoms of the alkyl side chains (of cations and anions confounded) is strong, denoting an ordering of alkyl tails pointing away from the metal surface. This is characteristic of segregation between the alkyl chains, which aggregate to form nonpolar regions, and the charged headgroups. In this ionic liquid, the second layer of anions appears less structured than in the first ionic liquid. Last, in  $[N_{1124}][C_4SO_3]$  the ordering of the alkyl tails is less prominent than in  $[N_{1124}][C_4SO_3]$ , an interesting effect of the ethyl group in the ammonium cation. The presence of this short alkyl chain attached to the cation headgroup seems to disrupt some of the segregation between charged and nonpolar moieties, clearly apparent when comparing plots b and c in Figure 5.

Color-labeling the atoms belonging to different functional groups of the ionic liquid allows visualization of the interfacial layer, depicted in Figure 6: anion headgroups (red) tend to reside closer to the surface followed by the alkylammonium head groups (blue) and finally the alkyl chains (black).

In order to analyze in detail the orientations of the ions at the interface, the position of the alkyl side chains with respect to the ionic head groups was plotted with the aid of a Legendre polynomial:

$$\langle P_2(\theta) \rangle = \left\langle \frac{1}{2} (3 \cos^2(\theta) - 1) \right\rangle \quad (2)$$

where  $\theta$  is the angle between the surface normal and a vector chosen in the ion. In the present ionic liquids, both cations and anions are composed of an essentially spherical headgroup (trimethylammonium or sulfonate) and an alkyl side chain; therefore, the vector representing the orientation of the ions was defined between a central atom of the cation or anion headgroup, i.e., N or S, and the terminal atom of the respective alkyl side chain, i.e.,  $C_S$  for  $[N_{1114}][C_1SO_3]$  or  $C_{3H}$  for  $[N_{1114}][C_4SO_3]$  and  $[N_{1124}][C_4SO_3]$ .  $P_2(\theta)$  varies from 1 to  $-0.5$ . A value of 1 indicates that the vector on the ion is parallel

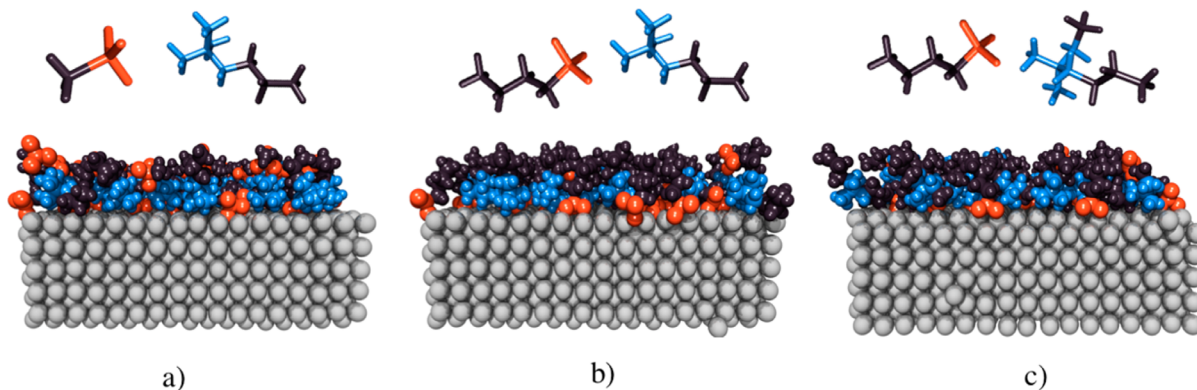


**Figure 6.** Snapshots of the metal–ionic liquid interface using color labeling: (a)  $[N_{1114}][C_1SO_3]$  and (b)  $[N_{1114}][C_4SO_3]$  and (c)  $[N_{1124}][C_4SO_3]$ . Red, blue, and black colors depict the sulfonfyl headgroups of anions, ammonium headgroups of cations, and alkyl chains of both ions, respectively.

to the surface normal, and therefore the alkyl side chains are perpendicular to the metal surface. A value of  $-0.5$  means that the vectors are perpendicular and the preferred orientation of the side chains is parallel to the metal surface. Figure 7 shows the preferred orientations of the cation (blue curves) and the anion (red curves) for the different ionic liquids in this study.

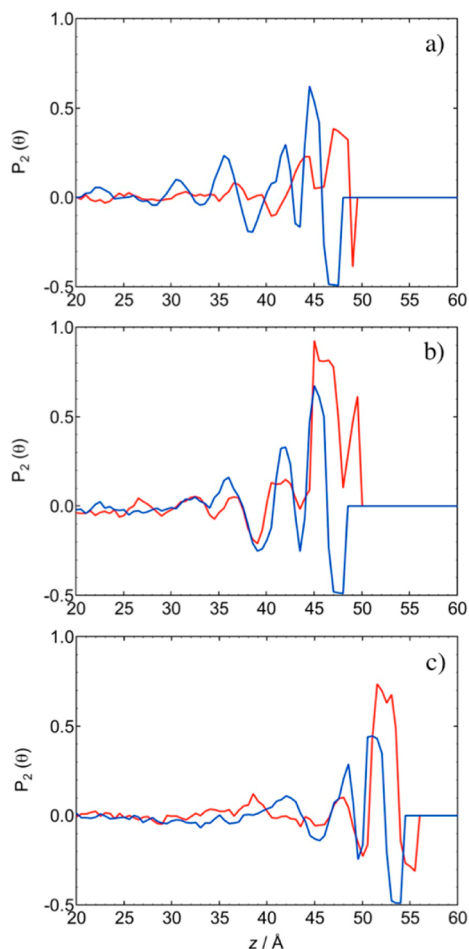


**Figure 7.** Orientational ordering parameter,  $P_2(\theta)$ , for the ionic liquids (a)  $[N_{1114}][C_1SO_3]$ , (b)  $[N_{1114}][C_4SO_3]$ , and (c)  $[N_{1124}][C_4SO_3]$ . The red curves represent the orientation of the anions and the blue curves, those of the cations.

For  $[N_{1114}][C_1SO_3]$ , there is a first negative peak corresponding to the  $C_S$  group in the anion of the first adsorbed layer that is oriented parallel to the metal surface. Then, for a length of  $1.5 \text{ \AA}$ , the  $C_S$  group will form an angle of around  $45^\circ$  with the surface, after which the orientation becomes random and  $P_2(\theta)$  decays to zero. In  $[N_{1114}][C_4SO_3]$ , the orientational order extends up to  $12 \text{ \AA}$  from the surface, and there are two pronounced peaks due to the anions separated by about  $3.5 \text{ \AA}$ , in agreement with the number-density profile for the  $C_{3H}$  atom (Figure 5a). The first of these peaks corresponds to an angle of  $\sim 50^\circ$  with the metal surface, while the second peak corresponds to a position quasi-perpendicular to this surface. Finally, for the anions of  $[N_{1124}][C_1SO_3]$ , the ordering of the alkyl chains decays at shorter lengths in comparison with the other two ionic liquids, in agreement with the density profiles presented in Figure 5. The first peak indicates the tendency of the  $S-C_{2H}-C_{2H}-C_{2H}-C_{3H}$  chain to adopt an orientation parallel toward the metal, followed by a second

layer in which the anions are mostly perpendicular. It is interesting to observe that, although there is only one methyl group differentiating  $[N_{1124}][C_4SO_3]$  from  $[N_{1114}][C_4SO_3]$ , the behaviors of the first layer of the alkyl side chains in the anions are opposite. In general, the anions adopt a perpendicular orientation in respect to the surface due to the strongly adsorbed oxygen atoms that render conformations parallel to the surface unfavorable.

The cation chains behave similarly in all three ionic liquids, being preferentially parallel to the surface for the first  $\sim 1 \text{ \AA}$ , after which, for  $2 \text{ \AA}$ , they lie at an average angle of  $35^\circ$  with the surface. This proximity of the cation side chains with the surface is the opposite of what is observed for the anions, likely because in the cation headgroups there are no specific interactions with Fe, as is the case of the oxygen atoms of the anions.

The thickness and structure of the electrostatic layer near the surface, resulting from the ordering of ions, can be seen in the plots of electrostatic charge distribution in Figure 8. The net charge in the liquid when moving away from the surface is first negative (due to the closest layer of anion headgroups) and then positive (due to the first layer of cations). In  $[N_{1114}][C_1SO_3]$ , a second negative peak is present as a result of the second layer of anions, which is still structured, in this ionic

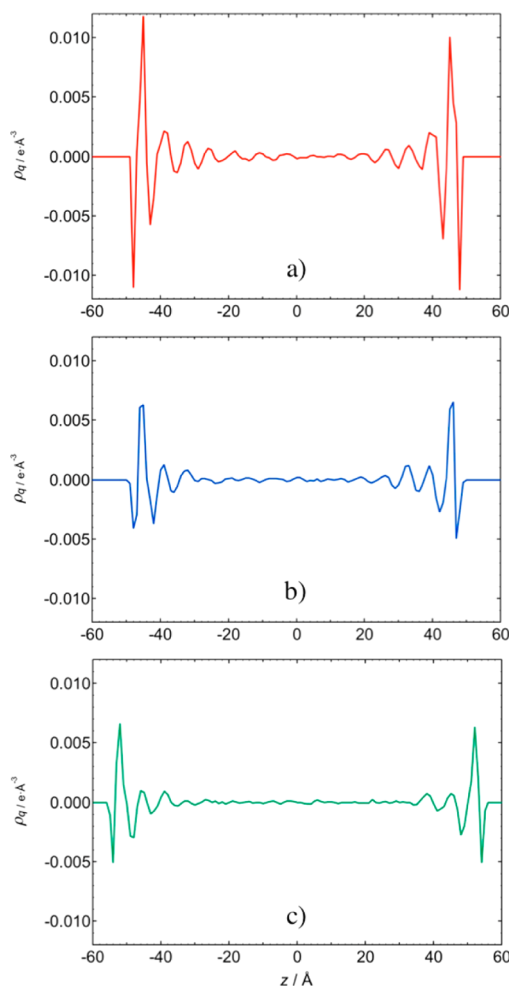


**Figure 8.** Plots of electrostatic charge distribution along the simulation box for the ionic liquids (a)  $[N_{1114}][C_1SO_3]$ , (b)  $[N_{1114}][C_4SO_3]$ , and (c)  $[N_{1124}][C_4SO_3]$ .



liquid. The interfacial layer is roughly one-ion-thick, extended between 5 and 10 Å into the liquid.

Spectroscopic studies of Baldelli<sup>31</sup> using vibrational sum frequency generation revealed the formation of an interfacial layer at a metal surface, which is one-ion-thick, with both anions and cations present at the surface; thus the present results agree with this general picture. Unfortunately, the study concentrates on the orientation of the imidazolium ring of the cations and provides no information on the orientation of the alkyl side chains.

A previous molecular simulation study using a model analogous to the one presented here,<sup>10</sup> but focusing on the structure of imidazolium bistriflamide ionic liquids solvating a metal nanoparticle, yielded the same overall pictures as the present work: an interfacial layer that is essentially one-ion-thick, with cation headgroups and anions in the vicinity of the surface and the alkyl side chains directed away from the nanoparticle. Simulations of molten salts at conducting surfaces, for spherical ions such as in LiCl,<sup>29</sup> also indicate the formation of one adsorbed layer (in the absence of an applied surface electrical potential) with charge fluctuations quickly screened into the liquid.

## CONCLUSIONS

In this work, we developed an interaction model between an ionic liquid and a metal surface based on quantum chemical calculations and including the polarization of the metal. The model is of the atom–atom type, and therefore it is independent of the surface topology and can be used to represent flat or rough surfaces. It can be combined with existing force-field models for ionic liquids and for metallic materials in order to simulate heterogeneous systems. Our specific treatment of the interactions between the sites of the ionic liquid and the metal surface, and including polarization of the conductor, produces a more reliable representation of the interactions than is possible using existing empirical and nonpolarizable force field models.

We studied the ordering of three alkylammonium alkylsulfonate ionic liquids—[N<sub>1114</sub>][C<sub>1</sub>SO<sub>3</sub>], [N<sub>1114</sub>][C<sub>4</sub>SO<sub>3</sub>], and [N<sub>1124</sub>][C<sub>4</sub>SO<sub>3</sub>—at an iron surface, in the context of developing environmentally acceptable ionic lubricants. The variations in the molecular structure of the ions allowed us to deduce relations between these structures and the interfacial layer of ionic liquid. The first conclusion is that both anions and cations are found in the interfacial layer, which is on the order of one-ion-thick, a result of the electrostatic screening of the ionic medium. This is in agreement with experimental results from the literature. Nonetheless, when the alkyl side chains are shorter in the anions, a second layer of anions with a significant ordering is observed. The charged headgroups lie close to the surface, with a predominance of the oxygen atoms of the anions that are strongly adsorbed. The role of the alkyl side chains in the cation and the anion are not similar: whereas the alkyl (butyl) side chains of the anions tend to point away from the surface, the butyl side chains of the first layer of ammonium cations tend to orient parallel to the surface. Therefore, there is a non-negligible interaction of the alkyl side chains and the iron surface.

These elements of information concerning the structure of the ionic liquids at metal surfaces contribute to improving our knowledge of tribological or electrochemical systems using these fluids. The models developed here will be used in nonequilibrium molecular dynamics simulations of systems

under shear, in order to study the impact of the molecular structures in the friction coefficient and to establish structure–property relations.

## AUTHOR INFORMATION

### Corresponding Author

\*Tel.: +33 (0)4 73 40 71 66. Fax: +33 (0)4 73 40 53 28. E-mail: agilio.padua@univ-bpclermont.fr.

### Notes

The authors declare no competing financial interest.

## ACKNOWLEDGMENTS

The present work was supported by the Marie Curie Initial Training Network MINILUBES (<http://www.minilubes.net/>) of the 7th Framework Program of the European Commission.

## REFERENCES

- (1) Lopes, J. N. C.; Pádua, A. A. H. *J. Phys. Chem. B* **2004**, *108*, 9.
- (2) Lopes, J. N. C.; Pádua, A. A. H. *J. Phys. Chem. B* **2004**, *108*, 16893.
- (3) Lopes, J. N. C.; Pádua, A. A. H. *J. Phys. Chem. B* **2006**, *110*, 7.
- (4) Lopes, J. N. C.; Pádua, A. A. H.; Shimizu, K. *J. Phys. Chem. B* **2008**, *112*, 5039.
- (5) Sambasivarao, S. V.; Acevedo, O. *J. Chem. Theory Comput.* **2009**, *5*, 1038.
- (6) Shimizu, K.; Almantariotis, D.; Gomes, M. F. C.; Pádua, A. A. H.; Lopes, J. N. C. *J. Phys. Chem. B* **2010**, *114*, 3592.
- (7) Borodin, O. *J. Phys. Chem. B* **2009**, *113*, 11463.
- (8) Bhargava, B. L.; Balasubramanian, S. *J. Chem. Phys.* **2007**, *127*.
- (9) Finnis, M. W.; Sinclair, J. E. *Philos. Mag. A* **1984**, *50*, 45.
- (10) Pensado, A. S.; Padua, A. A. H. *Angew. Chem., Int. Ed.* **2011**, *50*, 8683.
- (11) Stolte, S.; Steudte, S.; Igartua, A.; Stepnowski, P. *Curr. Org. Chem.* **2011**, *15*, 1946.
- (12) Stolte, S.; Steudte, S.; Areitioaurtena, O.; Pagano, F.; Thöming, J.; Stepnowski, P.; Igartua, A. *Chemosphere* **2012**.
- (13) Bermudez, M. D.; Jimenez, A. E.; Sanes, J.; Carrion, F. J. *Molecules* **2009**, *14*, 2888.
- (14) Chen, Q.; Zheng, S.; Yang, S.; Li, W.; Song, X.; Cao, B. *Sol-Gel Sci. Technol.* **2012**, *61*, 501.
- (15) Carrion, F. J.; Martinez-Nicolas, G.; Iglesias, P.; Sanes, J.; Bermudez, M. D. *Int. J. Mol. Sci.* **2009**, *10*, 4102.
- (16) Ye, C. F.; Liu, W. M.; Chen, Y. X.; Yu, L. G. *Chem. Commun.* **2001**, 2244.
- (17) Minami, I. *Molecules* **2009**, *14*, 2286.
- (18) Wasserscheid, P.; Welton, T. *Outlook*; Wiley-VCH Verlag GmbH & Co. KGaA: New York, 2003.
- (19) Pensado, A.; Comuñas, M.; Fernández, J. *Tribol. Lett.* **2008**, *31*, 107.
- (20) Jimenez, A. E.; Bermudez, M. D.; Carrion, F. J.; Martinez-Nicolas, G. *Wear* **2006**, *261*, 347.
- (21) Kamimura, H.; Kubo, T.; Minami, I.; Mori, S. *Tribol. Int.* **2007**, *40*, 620.
- (22) Qu, J.; Truhan, J. J.; Dai, S.; Luo, H.; Blau, P. J. *Tribol. Lett.* **2006**, *22*, 207.
- (23) Padua, A. A. H.; Lopes, J. *Abstr. Pap.—Am. Chem. Soc.* **2006**, *231*, 35.
- (24) Harrison, J. A.; Stuart, S. J.; Brenner, D. W. In *Handbook of Micro/Nanotribology*; Bhushan, B., Ed.; CRC Press: Boca Raton, FL, 1999; p 525.
- (25) Robbins, M. O.; Müser, M. H. In *Modern Tribology Handbook*; Bhushan, B., Ed.; CRC Press: Boca Raton, FL, 2001; p 717.
- (26) Shim, Y.; Kim, H. J. *ACS Nano* **2009**, *3*, 1693.
- (27) Shim, Y.; Jung, Y.; Kim, H. J. *J. Phys. Chem. C* **2011**, *115*, 23574.
- (28) Fedorov, M. V.; Lynden-Bell, R. M. *Phys. Chem. Chem. Phys.* **2012**, *14*, 2552.

- (29) Tazi, S.; Salanne, M.; Simon, C.; Turq, P.; Pounds, M.; Madden, P. A. *J. Phys. Chem. B* **2010**, *114*, 8453.
- (30) Salanne, M.; Madden, P. A. *Mol. Phys.* **2011**, *109*, 2299.
- (31) Baldelli, S. *Acc. Chem. Res.* **2008**, *41*, 421.
- (32) Kaminski, G.; Jorgensen, W. L. *J. Phys. Chem.* **1996**, *100*, 18010.
- (33) Jorgensen, W. L.; Maxwell, D. S.; TiradoRives, J. *J. Am. Chem. Soc.* **1996**, *118*, 11225.
- (34) Watanabe, Y.; Shibuta, Y.; Suzuki, T. *ISIJ Int.* **2010**, *50*, 1158.
- (35) Zhao, Y.; Truhlar, D. G. *J. Chem. Phys.* **2006**, 125.
- (36) Walker, P. D.; Mezey, P. G. *J. Am. Chem. Soc.* **1993**, *115*, 12423.
- (37) Frisch, M. J.; Trucks, G. W.; Schlegel, H. B.; Scuseria, G. E.; Robb, M. A.; Cheeseman, J. R.; Scalmani, G.; Barone, V.; Mennucci, B.; Petersson, G. A.; Nakatsuji, H.; Caricato, M.; Li, X.; Hratchian, H. P.; Izmaylov, A. F.; Bloino, J.; Zheng, G.; Sonnenberg, J. L.; Hada, M.; Ehara, M.; Toyota, K.; Fukuda, R.; Hasegawa, J.; Ishida, M.; Nakajima, T.; Honda, Y.; Kitao, O.; Nakai, H.; Vreven, T.; Montgomery, J. A., Jr.; Peralta, J. E.; Ogliaro, F.; Bearpark, M.; Heyd, J. J.; Brothers, E.; Kudin, K. N.; Staroverov, V. N.; Kobayashi, R.; Normand, J.; Raghavachari, K.; Rendell, A.; Burant, J. C.; Iyengar, S. S.; Tomasi, J.; Cossi, M.; Rega, N.; Millam, N. J.; Klene, M.; Knox, J. E.; Cross, J. B.; Bakken, V.; Adamo, C.; Jaramillo, J.; Gomperts, R.; Stratmann, R. E.; Yazyev, O.; Austin, A. J.; Cammi, R.; Pomelli, C.; Ochterski, J. W.; Martin, R. L.; Morokuma, K.; Zakrzewski, V. G.; Voth, G. A.; Salvador, P.; Dannenberg, J. J.; Dapprich, S.; Daniels, A. D.; Farkas, Ö.; Foresman, J. B.; Ortiz, J. V.; Cioslowski, J.; Fox, D. J. *Gaussian 09*; Gaussian, Inc.: Wallingford, CT, 2009.
- (38) Schafer, A.; Huber, C.; Ahlrichs, R. *J. Chem. Phys.* **1994**, *100*, 5829.
- (39) Dolg, M.; Wedig, U.; Stoll, H.; Preuss, H. *J. Chem. Phys.* **1987**, *86*, 2123.
- (40) Vosko, S. H.; Wilk, L.; Nusair, M. *Can. J. Phys.* **1980**, *58*, 1200.
- (41) Hay, P. J.; Wadt, W. R. *J. Chem. Phys.* **1985**, *82*, 270.
- (42) Hay, P. J.; Wadt, W. R. *J. Chem. Phys.* **1985**, *82*, 299.
- (43) Kohler, C.; Seifert, G.; Frauenheim, T. *Chem. Phys.* **2005**, *309*, 23.
- (44) Boys, S. F.; Bernardi, F. *Mol. Phys.* **1970**, *19*, 553.
- (45) Weaver, J. F.; Carlsson, A. F.; Madix, R. J. *Surf. Sci. Rep.* **2003**, *50*, 107.
- (46) Chia-Ling Kao, R. J. M. *Surf. Sci.* **2004**, *557*, 15.
- (47) Lee, K.; Morikawa, Y.; Langreth, D. C. *Phys. Rev. B: Condens. Matter* **2010**, *82*, 155461.
- (48) Wang, L.-S.; Wu, H.; Desai, S. R. *Phys. Rev. Lett.* **1996**, *76*, 4853.
- (49) Clarke, J. H. R.; Smith, W.; Woodcock, L. V. *J. Chem. Phys.* **1986**, *84*, 2290.
- (50) Iori, F.; Corni, S. *J. Comput. Chem.* **2008**, *29*, 1656.
- (51) Smith, W.; Forester, T. R. *DL\_POLY*, 2.20 ed.; Daresbury Laboratory: Cheshire, England, 2007.
- (52) Sanmartin Pensado, A.; Malfreyt, P.; Pádua, A. A. H. *J. Phys. Chem. B* **2009**, *113*, 14708.
- (53) Allen, M. P.; Tildesley, D. J. *Computer Simulation of Liquids*; Clarendon Press: Oxford, U. K., 1989.